

Research article

Open Access

## Benchmarking pK<sub>a</sub> prediction

Matthew N Davies\*<sup>†1</sup>, Christopher P Toseland<sup>†1</sup>, David S Moss<sup>2</sup> and Darren R Flower<sup>1</sup>

Address: <sup>1</sup>Edward Jenner Institute for Vaccine Research, Compton, Berkshire, RG20 7NN, UK and <sup>2</sup>School of Crystallography, Birkbeck College, Malet Street, London WC1E 7HX, UK

Email: Matthew N Davies\* - m.davies@mail.cryst.bbk.ac.uk; Christopher P Toseland - chris.toseland@jenner.ac.uk; David S Moss - d.moss@mail.cryst.bbk.ac.uk; Darren R Flower - darren.flower@jenner.ac.uk

\* Corresponding author †Equal contributors

Published: 02 June 2006

Received: 21 November 2005

BMC Biochemistry 2006, 7:18 doi:10.1186/1471-2091-7-18

Accepted: 02 June 2006

This article is available from: <http://www.biomedcentral.com/1471-2091/7/18>

© 2006 Davies et al; licensee BioMed Central Ltd.

This is an Open Access article distributed under the terms of the Creative Commons Attribution License (<http://creativecommons.org/licenses/by/2.0>), which permits unrestricted use, distribution, and reproduction in any medium, provided the original work is properly cited.

### Abstract

**Background:** pK<sub>a</sub> values are a measure of the protonation of ionizable groups in proteins. Ionizable groups are involved in intra-protein, protein-solvent and protein-ligand interactions as well as solubility, protein folding and catalytic activity. The pK<sub>a</sub> shift of a group from its intrinsic value is determined by the perturbation of the residue by the environment and can be calculated from three-dimensional structural data.

**Results:** Here we use a large dataset of experimentally-determined pK<sub>a</sub>s to analyse the performance of different prediction techniques. Our work provides a benchmark of available software implementations: MCCE, MEAD, PROPKA and UHBD. Combinatorial and regression analysis is also used in an attempt to find a consensus approach towards pK<sub>a</sub> prediction. The tendency of individual programs to over- or underpredict the pK<sub>a</sub> value is related to the underlying methodology of the individual programs.

**Conclusion:** Overall, PROPKA is more accurate than the other three programs. Key to developing accurate predictive software will be a complete sampling of conformations accessible to protein structures.

### Background

A proper understanding of protein pK<sub>a</sub> values is essential to a proper understanding of pH-dependent characteristics of protein function. If the pK<sub>a</sub> of a particular group is known then one can determine its protonation state at a given pH, helping to determine several important properties including protein solubility, protein folding and catalytic activity. Knowledge of the pK<sub>a</sub> values of the residues of an active site can help to identify the reaction mechanism of an enzyme or aid in the interpretation of experimental results [1-4]. The pK<sub>a</sub> value is  $-\log_{10}(K_a)$  where K<sub>a</sub>,

is the ionization constant, a measure of a titratable group's ability to donate a proton:

$$K_a = \frac{[H^+][A^-]}{[HA]} \quad (1)$$

The pK<sub>a</sub> value is therefore equal to the pH when there is an equal concentration of the protonated and deprotonated groups in solution. Each residue with a titratable group has a model or 'intrinsic' pK<sub>a</sub> value, defined as the pK<sub>a</sub> value when all the other groups are fixed in their neutral state. Ionizable groups may be divided into acidic, which

are neutral in their protonated state, and basic, which are positively charged in their protonated state. The protonated and the non-protonated forms of a residue can be very different chemically. In the case of His, the protonated form is hydrophilic and positively charged while the non-protonated form has a hydrophobic and aromatic character. Consequently the nature of the interaction made by an ionizable group may differ significantly at a pH above or below the  $pK_a$ .

Table 1 shows the intrinsic or 'model'  $pK_a$  values for all protein titratable groups [5]. However, in real protein-solvent systems, interactions between a residue and its environment will cause the titratable group's  $pK_a$  value to deviate from that of the model. Hence the intrinsic  $pK_a$  value,  $pK_{Model}$ , combined with the environmental perturbation,  $\Delta pK_a$ , describes the real  $pK_a$  value of a group [6-9].

$$pK_a = pK_{Model} + \Delta pK_a \quad (2)$$

The  $pK_a$  shift caused by the environment is not easily quantified. This is especially true of ionizable residues within protein active sites as they often have markedly higher or lower values than the intrinsic  $pK_a$  [5]. The three main factors that contribute towards environmental perturbation of the  $pK_a$  value are inter-molecular hydrogen bonding, the desolvation effect and Coulombic interactions. Previous studies have identified hydrogen bonding as the most important determinant of  $pK_a$  values [6]. The hydrogen bonding strength is both distance and angle dependent and therefore the extent of the perturbation is heavily dependent on the position of the interacting residues relative to each other. This is less of a factor with side chain hydrogen bonds than with main chain as the former is more flexible and therefore more likely to adopt an optimal orientation for hydrogen bond interactions. The desolvation effect is also important; this describes the energy that is required to move a group from a state of full solvation to a position within the folded protein. Desolvation effects within the protein interior preferentially increases the energies of the negatively-charged, base

forms, which will increase the  $pK_a$  value, while in the case of His, Lys and Arg, the desolvation preferentially increases the energy of the positively-charged, acid forms, which will decrease the  $pK_a$  values. The extent of the shift is dependent on the degree to which the group is buried within the protein. The third of the major factors, which may cause a  $pK_a$  shift, are Coulombic interactions between ionizable groups. The pair-wise interactions are dependent on the charges of the respective groups, but also on their location as only residues that are buried produce significant charge-charge interactions.

It is possible to predict the  $pK_a$  value of a given protein residue from three-dimensional structural data. The  $pK_a$  shift may be calculated from the difference in energy between the group's charged and neutral forms and added to the  $pK_{model}$  value to estimate its true value. Several different algorithms have been developed to generate predicted  $pK_a$  values based on structural data.

The majority of papers which have assessed the reliability of  $pK_a$  predictive algorithms have only examined a limited number of proteins, making an evaluation of their accuracy very difficult [6,10-13]. The largest of these [13] looked at 260 experimental  $pK_a$  values taken from 41 proteins. Here we use a large  $pK_a$  dataset of 100 proteins, which is more than double that of the most extensive previous paper [13], to analyse the predictive capabilities of the MCCE [14,15], MEAD [16], PROPKA [17] and UHBD [18] programs. The programs differ in their methodology and we assessed the merits of each. An enhanced approach to the problem of  $pK_a$  prediction is proposed.

## Results and discussion

Technical difficulties with the UHBD program, due to errors in the protonation of histidine residues, prevented the successful processing of all 100 proteins; in total only 43 could be completed. This led to the creation of two separate datasets, the Large dataset (containing 492 residues and excluding the UHBD program) and the Small Dataset (containing 280 residues and including the

**Table 1: Model  $pK_a$  values for all protein basic and acidic titratable groups. See reference 5.**

Titratable Group	$pK_{model}$ Value	No. in Study		Mean $pK_{exp}$ Value
		LARGE	SMALL	
N-Termini	7.5	-	-	-
C-Termini	3.8	-	-	-
Arg	12	1	1	-
Asp	4	143	112	3.5
Cys	9.5	11	4	6.6
Glu	4.4	126	105	4.3
His	6.3	130	24	6.4
Lys	10.4	57	23	9.6
Tyr	10	26	16	9.5

UHBD program). Several of the programs produced outliers, in some cases outside of the physically possible pH 0–14 range. Outliers were removed from the dataset using a variety of different parameters to see the effect upon the overall accuracy of prediction. Datasets were generated where all predicted values were lesser or greater than the intrinsic values by 3, 5, 7 and 10 pH units were removed as well a dataset where only physically possible values were included. This data is presented in Table 2 and Table 3. It may be seen from the data that in general the best results were obtained by using values within a range of 5 pH units. Using those parameters, 89 residues were removed from the Large dataset leaving 403 and 39 residues were removed from the Small dataset leaving 241 residues. It is unlikely that the pKa of a titratable residues can deviate more than 5 pH units from the residue's intrinsic value (see Table 1).

The majority of the outliers in both datasets were generated by the MEAD program, particularly when the PARCE force field was used. Considerably more residues are present within the +/- 1 unit bands for MCCE, UHBD and PROPKA. Thus there is a clear division between the performance of MEAD and that of the other programs. The

same trend may be seen in the Root Mean Squared Deviation (RMSD) values (Table 2, 3). PROPKA is more accurate for Asp, Glu, Lys and Tyr with RMSD values of 0.934, 0.849, 0.260 and 1.001 respectively. His is more accurately predicted by MCCE with an RMSD of 1.522. With respect to the Small dataset in Table 3, PROPKA is the best predictor for all residues except Glu and His, where UHBD performs best: RMSD of 0.442 and 0.494 respectively. The overall accuracy of each program to a level of <0.5 pK<sub>a</sub> units is 27% AMBER, 34% PARSE, 42% MCCE, 40% UHBD (242 dataset) and 48% PROPKA. When the error range is increased to <1 unit, the difference between the programs is more distinct: 56% AMBER, 56% PARSE, 71% MCCE, 67% UHBD (Small dataset) and 81% PROPKA (Table 4, 5). Scatter plots for each program are shown in Figure 1.

From a previous study [19], 39 carboxyl residues found within protein active sites were selected. These are shown in Table 6 [20–30]. The 27 Asp and 12 Glu residues have experimental values that differ from the model pKa value by at least 1 unit. Values for Asp and Glu range from 2.0 – 9.9 and 2.1 – 6.7 respectively. PROPKA and UHBD are distinct within the <0.5 and <1 unit error bands (Table 7),

**Table 2: Overview of the prediction accuracy of the Large Dataset (404 Residues) I. The table shows the RMSD values for each of the residues from the whole dataset and the dataset following removal of non-physical values and of all outliers outside of a range of 3, 5, 7 and 10 pH units. Figures marked in bold indicate significant results (P = 0.05).**

	AMBER COMPLETE	TRUE	WITHI N10	WITHI N7	WITHI N5	WITHI N3	PARSE COMPLETE	TRUE	WITHI N10	WITHI N7	WITHI N5	WITHI N3
ARG	*	*	*	*	*	*	*	*	*	*	*	*
ASP	2.698	1.928	2.513	1.495	1.354	1.273	3.743	1.729	2.251	1.837	1.25	1.106
CYS	*	*	*	*	*	*	*	*	*	*	*	*
GLU	1.885	1.466	1.616	1.62	1.42	1.026	3.175	1.48	1.841	1.681	1.442	1.034
HIS	3.691	2.171	3.016	2.281	2.022	1.417	3.691	2.122	2.997	2.293	1.993	1.465
LYS	1.244	1.263	1.263	1.263	1.122	0.84	25.78	1.162	1.162	1.162	0.991	0.741
TYR	2.739	2.195	2.195	2.195	1.939	1.516	3.163	2.143	2.143	2.143	1.882	1.481
	MCCE COMPLETE	TRUE	WITHI N10	WITHI N7	WITHI N5	WITHI N3	PROPK A COMPLETE	TRUE	WITHI N10	WITHI N7	WITHI N5	WITHI N3
ARG	*	*	*	*	*	*	*	*	*	*	*	*
ASP	2.024	1.774	2.032	1.79	1.534	1.242	1.301	1.041	1.313	1.301	<b>0.934</b>	0.806
CYS	*	*	*	*	*	*	*	*	*	*	*	*
GLU	1.642	1.255	1.335	1.296	1.259	0.97	1.011	0.851	0.994	0.997	<b>0.849</b>	0.611
HIS	4.503	1.736	2.598	2.104	<b>1.522</b>	1.718	1.865	1.586	1.819	1.631	<b>1.530</b>	1.551
LYS	1.137	1.125	1.125	1.125	1.005	1.129	0.417	0.412	0.412	0.412	<b>2.600</b>	0.423
TYR	5.426	2.643	2.634	2.643	1.668	1.593	2.225	1.551	1.551	1.551	<b>1.001</b>	1.049

#### Outliers

COMPLETE 0 removed  
 TRUE 52 removed  
 WITHIN 10 23 removed  
 WITHIN 7 27 removed  
 WITHIN 5 89 removed  
 WITHIN 3 110 removed

**Table 3: Overview of the prediction accuracy of the Small Dataset (242 Residues) I.** The table shows the RMSD values for each of the residues from the whole dataset and the dataset following removal of non-physical values and of all outliers outside of a range of 3, 5, 7 and 10 pH units. Figures marked in bold indicate significant results ( $P = 0.05$ ).

	AMBER COMPLETE	TRUE	WITHI N10	WITHI N7	WITHI N5	WITHI N3	PARSE COMPLETE	TRUE	WITHI N10	WITHI N7	WITHI N5	WITHI N3
ARG	*	*	*	*	*	*	*	*	*	*	*	*
ASP	2.078	1.787	2.079	2.077	1.691	1.781	3.774	1.582	2.142	1.912	1.53	1.267
CYS	*	*	*	*	*	*	*	*	*	*	*	*
GLU	1.641	1.416	1.603	1.603	1.294	1.047	3.041	1.474	1.71	1.71	1.334	1.051
HIS	2.786	1.689	1.689	1.689	1.347	1.118	2.736	1.809	1.81	1.81	1.488	1.402
LYS	1.291	1.29	1.291	1.291	1.291	1.291	1.278	1.278	1.278	1.278	1.278	1.278
TYR	2.06	1.297	1.297	1.297	1.933	0.766	2.368	1.262	1.262	1.262	1.871	0.792
	MCCE COMPLETE	TRUE	WITHI N10	WITHI N7	WITHI N5	WITHI N3	UHBD COMPLETE	TRUE	WITHI N10	WITHI N7	WITHI N5	WITHI N3
ARG	*	*	*	*	*	*	*	*	*	*	*	*
ASP	1.915	1.735	1.921	1.731	1.319	1.419	0.95	0.824	0.838	0.842	0.89	0.641
CYS	*	*	*	*	*	*	*	*	*	*	*	*
GLU	1.575	1.185	1.237	1.237	1.188	0.893	0.508	0.478	0.493	0.493	<b>0.442</b>	0.395
HIS	1.985	1.584	1.584	1.584	1.056	1.593	0.634	0.453	0.453	0.453	<b>0.494</b>	0.428
LYS	1.152	1.152	1.152	1.152	1.152	1.152	0.412	0.412	0.412	0.412	0.412	0.412
TYR	6.027	1.373	1.373	1.373	1.456	1.419	0.687	0.582	0.582	0.582	0.61	0.631
	PROPKA COMPLETE	TRUE	WITHI N10	WITHI N7	WITHI N5	WITHI N3						
ARG	*	*	*	*	*	*						
ASP	1.827	1.826	1.806	1.809	<b>0.879</b>	0.745						
CYS	*	*	*	*	*	*						
GLU	0.987	0.773	0.959	0.959	0.781	0.632						
HIS	2.235	2.11	2.11	2.11	1.724	2.172						
LYS	0.394	0.394	0.394	0.394	<b>0.394</b>	0.394						
TYR	1.533	0.992	0.991	0.991	<b>0.572</b>	1.011						

#### Outliers

COMPLETE 0 removed  
 TRUE 25 removed  
 WITHIN 10 11 removed  
 WITHIN 7 13 removed  
 WITHIN 5 34 removed  
 WITHIN 3 54 removed

with PROPKA performing best with an accuracy of 66.67% within the <1 unit band. However a large discrepancy exists between the <1 and <0.5 bands for all of the programs, with an approximate 50% drop in accuracy. For the Asp residues, PROPKA predicts far better than the other programs, with values of 37.04%, compared to 18.52% for MCCE and 0% for UHBD at the <0.5 level. However, for Glu residues program performance is closer, with values of 25 % for PARSE, MCCE and UHBD and 33% for AMBER and PROPKA at the <0.5 level. When the error level is extended to <1, PROPKA is far better, with a value of 83.33% compared to its nearest rivals UHBD, AMBER and PARSE with values of 50%. PROPKA shows

an accuracy of 85% to within 1 pKa unit for surface residues, whereas the same accuracy is limited to 53% with the MCCE program for buried residues, a considerable reduction. The accuracy values obtained for MCCE were also comparable with those that recently appeared on the program's website, which show an RMSD of 0.77 and an accuracy range of 98% within the <2 pH unit range and 84% accuracy within the <1 pH unit range [31].

Given the capacity of the predictive programs to under or over predict the true  $pK_a$  value (see Discussion), the possibility of using a consensus approach to integrate the various programs was investigated. Using the Small dataset,

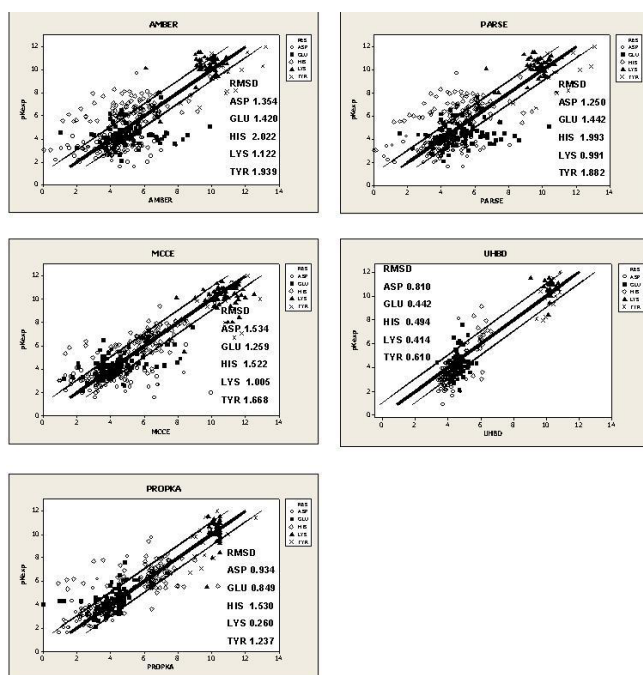


**Figure 1**  
**Correlation plots for the individual programs.** The bold line indicates perfect prediction ( $pK_{\text{pred}} = pK_{\text{exp}}$ ). The outer lines indicate  $\pm 1$  unit from the  $pK_{\text{exp}}$ .

combinations of the prediction values were calculated and the accuracy tested as before. From this dataset, 25 combinations (Table 8) were tried. One, UHBD + PROPKA, leads to improvements in all residues except histidine. The His RMSD value of 0.955, from this combination, is far better than all of the programs except UHBD, which has a value of 0.494. The overall accuracy of this combination was not a surprise due to the individual performance of each program. A further attempt to integrate the programs was made by using Partial Least Squared (PLS) regression. The PLS model generated had a correlation coefficient ( $r^2$ ) of 0.9 and a cross-validated correlation coefficient ( $q^2$ ) of 0.89. The resulting equations were applied to the Small dataset and the accuracy results are shown in Table 9. The accuracy improved greatly in the  $<0.5$  range to almost 58%, significantly greater than either the other programs run individually or the combination method (UHBD + PROPKA). Again, a disparity between the predictive capabilities of MEAD and the other programs may be seen. AMBER and PARSE have coefficients of -0.03129 and -0.0001836 respectively, which are comparatively small compared to the other coefficients (0.239, 0.4282 and 0.4108 for MCCE, UHBD and PROPKA respectively). The results above would indicate a more significant relationship between the PROPKA and UHBD predictions and the experimental  $pK_a$  values. This data fits with the trends seen in the other analysis. How-

ever, multiple linear regression is not an ideal way to increase predictive accuracy as combining programs will cause the propagation of experimental errors within a given dataset.

The disparity between the predictive capabilities of the program relates to the algorithm that used for the calculation. MEAD, UHBD and MCCE are all based upon an electrostatic continuum model that solves the linearised Poisson-Boltzmann equation numerically [32,33]. The electrostatic potential  $\phi(r)$  can be calculated by the Poisson-Boltzmann equation:

$$\nabla \epsilon(r) \nabla \phi(r) - \kappa^2(r) \epsilon(r) \phi(r) = -4\pi \rho(r) \quad (3)$$

Where  $\epsilon$  is the dielectric constant,  $r$  is the position vector,  $\Phi$  is the electrostatic potential,  $\rho$  is the charge distribution and  $\kappa$  is a parameter that represents the effect of mobile ions in solution. All three programs work on the assumption that the major determinant of the  $pK_a$  shift from the model values are the electrostatic effects of burying titratable groups in low dielectric medium. A model of the macromolecule-solvent system is used with dielectric constants of 80 for the solvent and 4 for the protein. The details of the atomic structure are incorporated into the placement of charges and dielectric boundaries. The calculation accounts for the desolvation energy, the titratable group's interaction with partial charges and the group's interaction with other titratable groups in the protein. MEAD consistently performs more poorly than the other two Poisson-Boltzmann-based programs. This may be because, in addition to the basic calculation, UHBD and MCCE also incorporate a Monte Carlo function to sample the multiple conformations of each titratable site. The Monte Carlo method achieves convergence by random sampling of side chain conformers. This allows the MCCE and UHBD programs to make a more realistic calculation of the charge-charge interactions than MEAD. The RMSD values of the two MEAD data sets – PARSE and AMBER – are comparable, both producing similar RMSD values and numbers of outliers. However, Table 2 shows that the PARSE force field generates outliers that deviate much further from the experimentally-determined values than those of AMBER. Although the parameters of the two force fields are similar; the atomic radii of the hydrogens for PARSE are slightly larger which may have created inaccurate charge-charge interactions that have increased the calculated  $pK_a$  value (this would also account for the program's propensity to generate outliers). This is especially noticeable for Lys where the respective RMSD values of AMBER and PARSE are 1.2 and 25.8.

Although the PROPKA and MCCE programs are of comparable accuracy, the data suggests that the former tends to under-predict  $pK_a$  values whilst the latter over-predicts

**Table 4: Overview of the prediction accuracy of the Large Dataset (404 Residues) II Three tables show the accuracy of the predictions to the measured  $pK_{exp}$  within the ranges of <2 to <0.5. This is taken as the number of residues predicted within each range. Figure marked in bold indicate significant results ( $P = 0.05$ ).**

TOTAL (404)								
	AMBER		PARSE		MCCE		PROPKA	
		%		%		%		%
<2	322	80	320	79	357	88	371	<b>92</b>
<1.5	283	70	282	70	328	81	354	<b>88</b>
<1	213	53	221	55	283	70	317	<b>78</b>
<0.5	108	27	139	34	168	42	195	<b>48</b>
SURFACE (337)								
	AMBER		PARSE		MCCE		PROPKA	
		%		%		%		%
<2	285	85	284	84	311	92	329	<b>98</b>
<1.5	255	76	253	75	290	86	317	<b>94</b>
<1	196	58	200	59	248	74	285	<b>85</b>
<0.5	98	29	132	39	151	45	184	<b>55</b>
BURIED (66)								
	AMBER		PARSE		MCCE		PROPKA	
		%		%		%		%
<2	37	56	36	55	46	<b>70</b>	42	64
<1.5	28	42	29	44	38	<b>58</b>	37	56
<1	17	26	21	32	35	<b>53</b>	32	48
<0.5	10	15	7	11	17	<b>26</b>	11	17

them (Figure 1). This observation may reflect the different approaches towards the calculation of the  $pK_a$  value in the two programs. PROPKA [17] takes a different approach to the other three programs, calculating the  $pK_a$  shift by using empirical rules that incorporate effects from hydrogen bonds, desolvation and Coulombic interactions. The

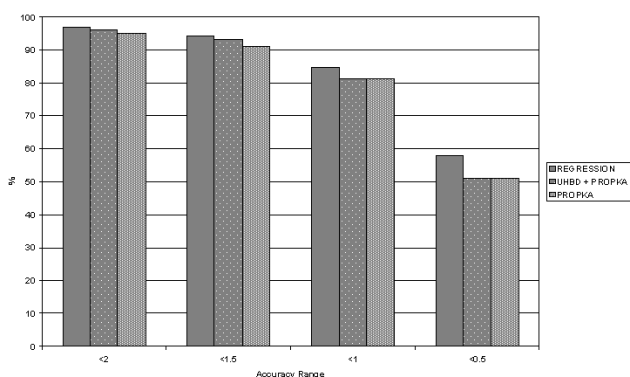


**Figure 2**  
**Comparative performance of the prediction methods.** The accuracy ranges (0.5 – 2) apply to the deviation from the measured  $pK_a$  value. The percentage score represents the number of residues predicted in each range.

extent of the  $pK_a$  shift caused by hydrogen bonding is proportional to the number of hydrogen bonds formed by the titratable group [19]. The desolvation effect is calculated from the solvent accessible surface and the 'depth of burial' (the distance of the group from the protein surface). Lastly, the strength of the Coulombic charge-charge interactions is dependent on the distance between the charges and on the state of the surrounding ionizable residues. This process, however, is only applied to buried pairs of ionizable residues. Therefore PROPKA's tendency to under-predict  $pK_a$  values may be caused by the program's emphasis on the dominance of hydrogen bonding in determining the extent of the shift. Hydrogen bonds have the effect of lowering  $pK_a$  values [34] and the predicted values may reflect that. Conversely, MCCE's tendency to over-predict may be the result of charge-charge interaction forcing an increase in the  $pK_a$  value. The majority of the over-predicted values are surface residues and, unlike PROPKA, the MCCE program does not take into account the lessened effects of charge-charge interactions when the respective residues are not buried within the protein interior. Consequently, PROPKA and MCCE tend to be more accurate for surface and buried residues respectively.

Side chains located at active sites are of particular interest as they often have unusually high or low  $pK_a$  values. In

**Table 5: Overview of the prediction accuracy of the Small Dataset (242 Residues) II. Three tables show the accuracy of the predictions to the measured  $pK_{exp}$ . This is taken as the number of residues predicted within each range. Figures marked in bold indicate significant results ( $P = 0.05$ ).**

TOTAL (242)	AMBER		PARSE		MCCE		UHBD		PROPKA	
		%		%		%		%		%
<2	195	81	191	79	216	89	225	93	230	95
<1.5	174	72	171	71	201	83	209	86	220	91
<1	131	54	135	56	172	71	161	67	195	81
<0.5	63	26	87	36	110	45	97	40	125	52

SURFACE (209)	AMBER		PARSE		MCCE		UHBD		PROPKA	
		%		%		%		%		%
<2	179	86	176	84	193	92	199	95	205	<b>98</b>
<1.5	163	78	159	76	181	87	186	89	199	<b>95</b>
<1	126	60	125	60	156	75	152	73	181	<b>87</b>
<0.5	60	29	83	40	100	48	94	45	122	<b>58</b>

BURIED (33)	AMBER		PARSE		MCCE		UHBD		PROPKA	
		%		%		%		%		%
<2	16	48	15	45	23	70	26	<b>79</b>	25	76
<1.5	11	33	12	36	20	61	23	<b>70</b>	21	64
<1	5	15	10	30	16	<b>48</b>	9	27	14	42
<0.5	3	9	4	12	16	<b>30</b>	3	9	3	9

some instances, the electrostatic charge of the active site can be radically different from that of the rest of the protein as a means to 'steer' a ligand towards the binding cleft [35]. For a program to work as an effective  $pK_a$  prediction tool it must be able to predict unusual  $pK_a$  values accurately. Generally speaking, the accuracy of prediction decreased the further the measured  $pK_a$  value was from the side chain's intrinsic  $pK_a$ . Again, PROPKA proved to be the most consistent of the programs. This is not surprising as the design of the model and assignment of parameters were based upon a large dataset of carboxyl  $pK_a$  values. Overall, the active site data was encouraging at the <1 unit level. However, once reduced to <0.5, the accuracy of all of the programs decreased. This highlights a key area for the development of new models and programs.

An interesting correlation is seen with respect to the regression coefficients and the general performance of the programs. Coefficients are generally an indicator of the relative importance of the contributing terms in a regression equation. The comparative performance of PROPKA, the combination methods and the regression model is seen in Figure 2. PROPKA is equally effective as these additional methods, although the regression data per-

forms better than the best combination. A Molecular Dynamics simulation of one of the proteins from the dataset (Barnase wild type ribonuclease (*pdb* code: 1A2P)) showed a standard deviation of  $\pm 1.4$  for the  $pK_a$  value over a one-nanosecond period. This indicates that a dynamic structure has a large capacity for extreme  $pK_a$  shifts. This suggests that any accurate prediction  $pK_a$  method would need to incorporate conformational variability into the algorithm.

### Conclusion

PROPKA is the most accurate method for all residues except Glu and His, where it is narrowly surpassed by UHBD and MCCE, respectively. Furthermore, the program also produces by far the best values for surface residues, most likely by taking sufficient account of hydrogen bonding. However, MCCE predicts buried residues far better than PROPKA, possibly by a more accurate evaluation of the charge-charge interaction with the conformers optimised by the Monte Carlo procedure. It must be noted that in all cases, the prediction of the buried residues is less accurate than for surface residues, indicating it is easier to calculate the interaction of a solvated or partially solvated residue than one densely packed within the pro-

**Table 6: Carboxyl sites of interest. B = Buried, S = Surface. Figures marked in bold indicate predictions >2 units from the  $pK_{exp}$ .**

PDB	RESIDUE	LOCATIO N	AMBER	PARSE	MCCE	UHBD	PROPKA	$pK_{exp}$
1A2P <sup>20</sup>	ASP-101	S	<b>6.19</b>	3.56	2.31	3.75	1.20	2.00
	ASP-93	S	<b>-0.64</b>	<b>-1.38</b>	1.00	3.92	0.69	2.00
	ASP-54	S	0.74	0.82	1.34	3.57	2.70	2.00
	GLU-73	B	<b>4.66</b>	4.10	2.37	<b>4.68</b>	3.11	2.10
1A91 <sup>21</sup>	ASP-7	S	3.99	<b>20.29</b>	4.17	4.04	3.87	5.60
	ASP-44	S	6.00	<b>20.22</b>	5.55	4.69	4.19	5.60
	ASP-61	S	5.52	<b>26.20</b>	5.01	<b>4.33</b>	<b>4.01</b>	7.00
	GLU-2	S	4.14	7.45	4.53	4.45	4.50	5.50
1BEO <sup>22</sup>	GLU-37	S	5.15	<b>-20.96</b>	4.27	4.66	4.32	5.50
	ASP-21	S	<b>6.38</b>	<b>5.52</b>	3.11	3.75	1.35	2.50
	ASP-30	S	3.56	3.80	4.38	4.00	2.64	2.50
1DE3 <sup>23</sup>	ASP-72	S	3.84	3.95	3.69	4.34	3.30	2.60
	GLU-96	B	<b>9.88</b>	<b>10.41</b>	3.53	5.70	4.10	5.10
	GLU-115	S	5.19	5.23	3.81	4.45	4.50	4.90
1KX1 <sup>24</sup>	ASP-59	S	3.13	3.90	2.33	4.20	2.49	2.30
1LZ3 <sup>25</sup>	ASP-18	S	3.79	3.94	<b>6.77</b>	4.05	3.19	2.70
	ASP-48	S	3.57	3.17	<b>5.15</b>	3.99	2.51	2.50
	ASP-66	S	0.23	<b>-0.31</b>	<b>12.38</b>	3.07	1.19	2.00
	ASP-87	S	4.06	3.96	<b>4.89</b>	3.89	2.17	2.10
	GLU-7	S	3.92	3.44	<b>4.73</b>	4.36	3.01	2.70
	GLU-35	B	4.92	5.23	7.80	4.78	5.40	6.10
1RNZ <sup>26</sup>	ASP-14	B	<b>9.08</b>	<b>7.86</b>	3.51	<b>4.89</b>	<b>-0.62</b>	2.00
	GLU-2	B	<b>-1.52</b>	<b>-1.48</b>	1.44	<b>5.03</b>	2.66	2.80
1TRS <sup>27</sup>	ASP-26	B	6.18	<b>4.38</b>	7.84	<b>4.64</b>	<b>4.96</b>	8.10
	GLU-6	S	3.91	3.92	4.54	4.44	4.50	4.90
	GLU-68	S	4.27	4.24	4.59	4.55	4.57	5.10
1TRW <sup>27</sup>	ASP-26	B	8.23	<b>5.24</b>	8.63	<b>4.83</b>	<b>5.62</b>	9.90
	GLU-68	S	5.07	5.33	3.55	4.88	4.34	4.90
1XNB <sup>28</sup>	ASP-11	S	1.83	0.57	3.44	3.82	1.99	2.50
	ASP-83	B	<b>6.29</b>	<b>7.89</b>	6.35	<b>4.28</b>	1.36	2.00
	ASP-101	B	<b>5.01</b>	2.94	<b>9.96</b>	<b>4.28</b>	1.50	2.00
	ASP-106	S	<b>8.72</b>	<b>8.94</b>	3.18	<b>4.98</b>	3.02	2.70
	GLU-172	B	6.62	6.42	5.94	5.22	7.32	6.70
2OVO <sup>29</sup>	ASP-7	S	4.05	4.01	<b>6.25</b>	3.72	2.51	2.50
	ASP-27	S	2.08	2.32	2.77	3.77	2.39	2.50
2RN2 <sup>30</sup>	ASP-10	B	<b>4.01</b>	<b>3.38</b>	<b>8.47</b>	<b>3.83</b>	6.99	6.10
	ASP-70	B	4.11	3.55	3.15	3.50	4.10	2.60
	ASP-102	B	<b>7.33</b>	<b>6.77</b>	3.00	3.40	0.13	2.00
	ASP-148	B	-1.10	<b>-1.31</b>	0.55	3.79	<b>-0.79</b>	2.00

tein interior. Overall, the best standalone program is PROPKA, which also produced the fewest outliers and is computationally much faster than the other programs. What the program lacks is a capacity to fully explore the conformational space available to the protein, which may ultimately limit its capacity to predict  $pK_a$  value. The reliability of the predictive programs tends to vary with both the residue type and its spatial location. For glutamic acid residues, UHBD produced the best results while for Histidine and for all buried residues, MCCE performed well. The comparatively poor prediction of the 'unusual'  $pK_a$  values by all of the programs was disappointing. Their ability to only predict a third of the residues to a high degree of accuracy highlights an area requiring further development. The variation in  $pK_a$  values observed in our

molecular dynamics simulation strongly suggests a complete sampling of conformations accessible to protein structures may be useful in creating accurate predictive software.

## Methods

100 proteins for which  $pK_a$  values had been determined experimentally were taken from PPD, a database of protein ionization constants [36,37]. The full list of the *pdb* files comprising the dataset is included as an additional file [See PDB codes]. A wide range of both protein size and function was represented in the dataset. The protein structures were taken from the RCSB protein data bank [38]. In order to run the MEAD program, *pdb* files were protonated by using the *leap* program and the AMBER 94 force field



**Table 7: Accuracy of prediction for the carboxyl sites. The accuracy was tested to the <2 to <0.5 ranges. The individual accuracy of the residues is given in the bottom two tables. Figures marked in bold indicate the greatest accuracy.**

TOTAL (242)	AMBER		PARSE		MCCE		UHBD		PROPKA	
		%		%		%		%		%
<2	26	66.67	20	51.28	30	76.92	30	76.92	34	<b>87.18</b>
<1.5	19	48.72	15	38.46	25	64.10	20	51.28	32	<b>82.05</b>
<1	10	25.64	10	25.64	17	43.59	8	20.51	26	<b>66.67</b>
<0.5	6	15.38	4	10.26	8	20.51	3	7.69	14	<b>35.90</b>

SURFACE (209)	AMBER		PARSE		MCCE		UHBD		PROPKA	
		%		%		%		%		%
<2	17	62.96	13	48.15	10	70.37	19	70.37	22	<b>81.48</b>
<1.5	10	37.04	8	29.63	16	59.26	11	40.74	20	<b>74.07</b>
<1	4	14.81	4	14.81	12	44.44	2	7.41	16	<b>59.26</b>
<0.5	2	7.41	1	3.70	5	18.52	0	0.00	10	<b>37.04</b>

BURIED (33)	AMBER		PARSE		MCCE		UHBD		PROPKA	
		%		%		%		%		%
<2	9	75.00	9	75.00	11	91.67	11	91.67	12	<b>100.00</b>
<1.5	9	75.00	7	58.33	9	75.00	9	75.00	12	<b>100.00</b>
<1	6	50.00	6	50.00	5	41.67	6	50.00	10	<b>83.33</b>
<0.5	4	<b>33.00</b>	3	25.00	3	25.00	3	25.00	4	<b>33.33</b>

(subsequent versions of the force field proved to be incompatible) and changed into *pqr* format using the online PDB2PQR converter [39,40]. Separate sets of files were created based on the AMBER99 and PARSE force fields. MEAD and UHBD were run on an IBM Blade Center Cluster, which consists of 5 Blade Centers containing 67 Dual Xeon (3.06Ghz, 1Gb) Blades. The MCCE calculations were carried out on an SG Octane. The majority of the *pdb* files did not need any modification. However, 1D3K, 1GU8, 1HRH and 1DRH were protonated with the *leap* program and the AMBER 03 force field in order to remove inconsistencies in the *pdb* files. Additionally, 1DUK, 1NFN and 2CI2 underwent minimization with *sander* using a steepest descent method that continued for 20,000 1 fs time steps or until the root mean square deviation between successive time-steps had fallen below 0.01Å in order to eliminate steric clashes. The PROPKA program was run online from its server [41]; no modification was required to run the files. Values for all Asp, Glu, His, Tyr, Lys residues were predicted. Arg was excluded from the calculation due to lack of experimental data. Arginines's high pK<sub>a</sub> precludes establishing a titratable

curve as the protein denatures at high pH. Cys was also excluded from the calculations due to a lack of experimental data.

The resultant data was also analysed using the Partial Least Squares (PLS) method. PLS is an extension of Multiple Linear Regression (MLR) that where a set of coefficients are developed from dependent variables, in this case the pK<sub>a</sub> prediction values, by comparison with the independent variables, the experimental pK<sub>a</sub> values. The PLS analysis was performed using the program GOLPE (Generating Optimal Linear PLS Estimations)[42].

#### Authors' contributions

MND formatted the data carried out the calculations for all of the pK<sub>a</sub> programs mentioned. CPT assembled the data set and carried out statistical analysis on the output of the pK<sub>a</sub> programs. DSM supervised the pK<sub>a</sub> calculations using the MEAD and UHBD programs at Birkbeck College. DRF instigated and supervised the entire project. MND, CPT and DRF drafted the manuscript. All authors have read and accepted the manuscript.

**Table 8: Overview of the combination methods (242 Residues). The residue RMSD values are given for all of the 25 combinations consisting of AMBER (A), PARSE (P), MCCE (M), UHBD (U) and PROPKA (P). Figures marked in bold indicate an improvement while the asterisk indicates the best score.**

	A + P	A + M	A + U	A + PR	P + M
ASP	1.556	1.245	1.174	<b>0.837</b>	1.161
GLU	1.301	1.012	0.816	0.676	1.026
HIS	1.331	0.631	0.827	1.000	0.727
LYS	1.281	0.763	0.742	0.646	0.793
TYR	1.899	1.512	1.238	1.028	1.502
	P + U	P + PR	M + U	M + PR	U + PR
ASP	1.074	<b>0.786</b>	0.910	<b>0.818</b>	<b>0.596</b>
GLU	0.834	0.690	0.660	0.766	<b>0.393</b>
HIS	0.812	0.987	0.566	1.289	0.955
LYS	0.742	0.647	0.713	0.755	<b>0.366</b>
TYR	1.212	1.016	0.974	0.956	<b>0.466</b>
	A + P + M	A + P + U	A + P + PR	A + M + U	A + M + PR
ASP	1.262	1.242	1.000	1.038	<b>0.837</b>
GLU	1.064	0.973	0.844	0.761	0.714
HIS	0.792	0.954	0.942	0.520	0.839
LYS	0.868	0.913	0.846	0.615	0.590
TYR	1.607	1.446	1.300	1.195	1.097
	A + U + PR	P + M + U	P + M + PR	M + U + PR	A + P + M + U
ASP	<b>0.773</b>	0.972	<b>0.795</b>	<b>0.681</b>	1.101
GLU	0.539	0.770	0.720	0.529	0.870
HIS	0.771	0.523	0.840	0.897	0.646
LYS	0.518	0.634	0.610	0.597	0.718
TYR	0.869	1.188	1.098	0.782	1.345
	A + P + M + PR	A + P + U + PR	A + M + U + PR	P + M + U + PR	A + P + M + U + PR
ASP	0.929	0.905	<b>0.779</b>	<b>0.738</b>	<b>0.866</b>
GLU	0.798	0.706	0.588	0.592	0.690
HIS	0.754	0.771	0.690	0.668	0.650
LYS	0.683	0.689	0.525	0.540	0.605
TYR	1.256	1.112	0.959	0.959	1.115

**Table 9: Accuracy of the multiple regression. The accuracy is given as the number of predictions within a range of the  $pK_{exp}$ . For comparison the UHBD + PROPKA combination is added. Figures marked in bold indicate improvements.**

TOTAL (242)	REGRESSION		UHBD + PROPKA	
		%		%
<2	234	96.69	233	96
<1.5	228	<b>94.21</b>	226	93
<1	205	<b>84.71</b>	197	81
<0.5	140	<b>57.85</b>	124	51

## Additional material

### Additional File 1

PDB codes, a full list of the pdb codes for the three-dimensional structures comprising the dataset.

Click here for file

[<http://www.biomedcentral.com/content/supplementary/1471-2091-7-18-S1.doc>]

## Acknowledgements

We should like to thank Dr Channa Hattotuwegama, Dr David Houlder-shaw and Dr Andy Purkiss for their helpful advice and assistance. The Edward Jenner Institute for Vaccine Research wishes to thank its sponsors: GlaxoSmithKline, the Medical Research Council, the Biotechnology and Biological Sciences Research Council, and the UK Department of Health.

## References

- Raquet X, Lounnas V, Lamotte-Brasseur J, Frere JM, Wade RC: **pK<sub>a</sub> calculations for class A beta-lactamases: methodological and mechanistic implications.** *Biophys J* 1997, **73**:2416-26.
- Lamotte-Brasseur J, Lounnas V, Raquet X, Wade RC: **pK<sub>a</sub> calculations for class A beta-lactamases: influence of substrate binding.** *Protein Sci* 1999, **8**:404-9.
- Lamotte-Brasseur J, Dubus A, Wade RC: **pK<sub>a</sub> calculations for class C beta-lactamases: the role of Tyr-150.** *Proteins* 2000, **40**:23-8.
- Nielsen JE, McCammon JA: **Calculating pK<sub>a</sub> values in enzyme active sites.** *Protein Sci* 2003, **12**:1894-901.
- Warshel A: **Calculations of enzymatic reactions: Calculations of pK<sub>a</sub> proton transfer reactions, and general acid catalysis reactions in enzymes.** *Biochemistry* 1981, **20**:3167-3177.
- Mehler EL, Guarnieri F: **A self-consistent, microenvironment modulated screened coulomb potential approximation to calculate pH-dependent electrostatic effects in proteins.** *Biophys J* 1999, **77**:3-22.
- Edgcomb SP, Murphy KP: **Variability in the pK<sub>a</sub> of His side-chains correlates with burial within proteins.** *Proteins* 2002, **49**:1-6.
- Harris TK, Turner GJ: **Structural basis of perturbed pK<sub>a</sub> values of catalytic groups in enzyme active sites.** *IUBMB Life* 2002, **53**:85-98.
- Li H, Robertson AD, Jensen JH: **The determinants of carboxyl pK<sub>a</sub> values in turkey ovomucoid third domain.** *Proteins* 2004, **55**:689-704.
- Demchuk E, Wade RC: **Improving the continuum dielectric approach to calculating pK<sub>s</sub> of ionizable groups in proteins.** *J Phys Chem* 1996, **100**:17373-17387.
- Nielsen JE, Vriend G: **Optimizing the hydrogen-bond network in Poisson-Boltzmann equation-based pK<sub>a</sub> calculations.** *Proteins* 2001, **43**:403-412.
- Georgescu RE, Alexov EG, Gunner MR: **Combining conformational flexibility and continuum electrostatics for calculating pK<sub>s</sub> in proteins.** *Biophys J* 2002, **83**:1731-1748.
- Wisiz MS, Hellinga HW: **An empirical model for electrostatic interactions in proteins incorporating multiple geometry-dependent dielectric constants.** *Proteins* 2003, **51**:360-377.
- Alexov EG, Gunner MR: **Incorporating protein conformational flexibility into the calculation of pH-dependent protein properties.** *Biophys J* 1997, **72**:2075-2093.
- Alexov EG, Gunner MR: **Calculated protein and proton motions coupled to electron transfer: electron transfer from QA- to QB in bacterial photosynthetic reaction centers.** *Biochemistry* 1999, **38**:8253-8270.
- Bashford D: **An object-oriented programming suite for electrostatic effects in biological molecules.** *Scientific Computing in Object-Oriented Parallel Environments* 1997, **1343**:233-240.
- Li H, Robertson AD, Jensen JH: **Very Fast Empirical Prediction and Rationalization of Protein pK<sub>a</sub> values.** *Proteins* 2005, **55**:689-704.
- Madura JD, Briggs JM, Wade RC, Davis ME, Luty BA, Ilin A, Antosiewicz J, Gilson MK, Bagheri B, Scott LR, McCammon JA: **Electrostatics and Diffusion of Molecules in Solution: Simulations with the University of Houston Brownian Dynamics Program.** *Comp Phys Comm* 1995, **91**:57-95.
- Forsyth WR, Antosiewicz JM, Robertson AD: **Empirical relationships between protein structure and carboxyl pK<sub>a</sub> values in proteins.** *Proteins* 2002, **48**:388-403.
- Oliveberg M, Arcus VL, Fersht AR: **pK<sub>a</sub> values of carboxyl groups in the native and denatured states of barnase: the pK<sub>a</sub> values of the denatured state are on average 0.4 units lower than those of model compounds.** *Biochemistry* 1995, **134**:9424-9433.
- Assadi-Porter FM, Fillingame RH: **Proton-translocating carboxyl of subunit c of F1Fo H(+)-ATP synthase: the unique environment suggested by the pK<sub>a</sub> determined by 1H NMR.** *Biochemistry* 1995, **34**:16186-16193.
- Gooley PR, Keniry MA, Dimitrov RA, Marsh DE, Keizer DW, Gayler KR, Grant BR: **The NMR solution structure and characterization of pH dependent chemical shifts of the beta-elicitin, cryptogein.** *J Biomol NMR* 1998, **12**:523-534.
- Perez-Canadillas JM, Campos-Olivas R, Lacadena J, Martinez del Pozo A, Gavilanes JG, Santoro J, Rico M, Bruix M: **Characterization of pK<sub>a</sub> values and titration shifts in the cytotoxic ribonuclease alpha-sarcin by NMR. Relationship between electrostatic interactions, structure, and catalytic function.** *Biochemistry* 1998, **37**:15865-15876.
- Chiang CM, Chang SL, Lin HJ, Wu WG: **The role of acidic amino acid residues in the structural stability of snake cardiotoxins.** *Biochemistry* 1996, **35**:9177-9186.
- Bartik K, Redfield C, Dobson CM: **Measurement of the individual pK<sub>a</sub> values of acidic residues of hen and turkey lysozymes by two-dimensional 1H NMR.** *Biophys J* 1994, **66**:1180-1184.
- Cohen JS, Griffin JH, Schechter AN: **Nuclear magnetic resonance titration curves of histidine ring protons. IV. The effects of phosphate and sulfate on ribonuclease.** *J Biol Chem* 1973, **248**:4305-4310.
- Qin J, Clore GM, Gronenborn AM: **Ionization equilibria for side-chain carboxyl groups in oxidized and reduced human thioredoxin and in the complex with its target peptide from the transcription factor NF kappa B.** *Biochemistry* 1996, **35**:7-13.
- Joshi MD, Hedberg A, McIntosh LP: **Complete measurement of the pK<sub>a</sub> values of the carboxyl and imidazole groups in Bacillus circulans xylanase.** *Protein Sci* 1997, **6**:2667-2670.
- Schaller W, Robertson AD: **pH, ionic strength, and temperature dependences of ionization equilibria for the carboxyl groups in turkey ovomucoid third domain.** *Biochemistry* 1995, **34**:4714-4723.
- Oda Y, Yamazaki T, Nagayama K, Kanaya S, Kuroda Y, Nakamura H: **Individual ionization constants of all the carboxyl groups in ribonuclease HI from Escherichia coli determined by NMR.** *Biochemistry* 1994, **33**:5275-84. [<http://www.sci.cny.cuny.edu/~mce/>].
- Nicholls A, Honig B: **A rapid finite difference algorithm, utilizing successive over-relaxation to solve the Poisson-Boltzmann equation.** *J Comput Chem* 1991, **12**:435-445.
- Rocchia W, Alexov E, Honig B: **Extending the applicability of the nonlinear Poisson-Boltzmann equation: Multiple dielectric constants and multivalent ions.** *J Phys Chem* 2001, **105**:6507-6514.
- Rocchia W, Sridharan S, Nicholls A, Alexov E, Chiabrera A, Honig B: **Rapid Grid-based Construction of the Molecular Surface for both Molecules and Geometric Objects: Applications to the Finite Difference Poisson-Boltzmann Method.** *J Comp Chem* 2002, **23**:128-137.
- Bashford D, Gerwert K: **Electrostatic calculations of the pK<sub>a</sub> values of ionizable groups in Bacteriorhodopsin.** *J Mol Biol* 1992, **224**:473-486.
- Toseland CP, McSparron H, Flower DR: **PPD v1.0 – An integrated, web-accessible database of protein ionization constants.** *Nucleic Acids Res* 2006, **34**:199-203. [<http://www.jenner.ac.uk/PPD/>].
- [<http://www.rcsb.org/pdb/>].
- Dolinsky TJ, Nielsen JE, McCammon JA, Baker NA: **PDB2PQR: an automated pipeline for the setup of Poisson-Boltzmann electrostatics calculations.** *Nucleic Acids Res* 2004, **32**:665-667. [<http://agave.wustl.edu/pdb2pqr/>].

41. [<http://ghemical.chem.uiowa.edu/>].
42. **GOLPE 4.5.** *Multivariate Infometric Analysis Srl, Viale dei Castagni 16, Perugia, Italy; 1999.*

Publish with **BioMed Central** and every scientist can read your work free of charge

*"BioMed Central will be the most significant development for disseminating the results of biomedical research in our lifetime."*

Sir Paul Nurse, Cancer Research UK

Your research papers will be:

- available free of charge to the entire biomedical community
- peer reviewed and published immediately upon acceptance
- cited in PubMed and archived on PubMed Central
- yours — you keep the copyright

Submit your manuscript here:  
[http://www.biomedcentral.com/info/publishing\\_adv.asp](http://www.biomedcentral.com/info/publishing_adv.asp)

